Hard X-ray emission in the star-forming region ON 2: discovery with *XMM-Newton*.

L. M. Oskinova

Institute for Physics and Astronomy, University of Potsdam, 14476 Potsdam, Germany

lida@astro.physik.uni-potsdam.de

R. A. Gruendl

Department of Astronomy, University of Illinois, 1002 West Green Street, Urbana, IL 61801, USA

R. Ignace

Department of Physics and Astronomy, East Tennessee State University, Johnson City, TN 37614, USA

Y.-H. Chu

Department of Astronomy, University of Illinois, 1002 West Green Street, Urbana, IL 61801, USA

W.-R. Hamann

Institute for Physics and Astronomy, University of Potsdam, 14476 Potsdam, Germany

A. Feldmeier

Institute for Physics and Astronomy, University of Potsdam, 14476 Potsdam, Germany

ABSTRACT

We obtained X-ray *XMM-Newton* observations of the open cluster Berkeley 87 and the massive star-forming region (SFR) ON 2. In addition, archival infrared *Spitzer Space Telescope* observations were used to study the morphology of ON 2, to uncover young stellar objects, and to investigate their relationship with the X-ray sources. It is likely that the SFR ON 2 and Berkeley 87 are at the same distance, 1.23 kpc, and hence are associated. The *XMM-Newton* observations detected X-rays from massive stars in Berkeley 87 as well as diffuse emission from the SFR ON 2. The two patches of diffuse X-ray emission are encompassed in the shell-like H II region GAL 75.84+0.40 in the northern part of ON 2 and in the ON 2S region in the southern part of ON 2. The diffuse emission from GAL 75.84+0.40 suffers an absorption column equivalent to $A_\mathrm{V} \approx 28$ mag. Its spectrum can be fitted either with a thermal plasma model at $T \gtrsim 30$ MK or by an absorbed power-law model with $\gamma \approx -2.6$. The X-ray luminosity of GAL 75.84+0.40 is $L_\mathrm{X} \approx 1 \times 10^{32}$ erg s^{-1}. The diffuse emission from ON 2S is adjacent to the ultra-compact H II (UCH II) region Cygnus 2N, but does not coincide with it or with any other known UCH II region. It has a luminosity of $L_\mathrm{X} \approx 6 \times 10^{31}$ erg s^{-1}. The spectrum can be fitted with an absorbed power-law model with $\gamma \approx -1.4$. We adopt the view of Turner & Forbes (1982) that the SFR ON 2 is physically associated with the massive star cluster Berkeley 87 hosting the WO type star WR 142. We discuss different explanations for the apparently diffuse X-ray emission in these SFRs. These include synchrotron radiation, invoked by the co-existence of strongly shocked stellar winds and turbulent magnetic fields in the star-forming complex, cluster wind emission, or an unresolved population of point sources.

Subject headings: H II regions – open clusters and associations: individual (Berkeley 87) – stars: early-type – stars: winds, outflows – X-rays: ISM – X-rays: stars

1. Introduction

Recent observational advances in X-ray astrophysics have led to a new high-energy perspective on the interstellar medium and star-forming regions (SFRs). The X-ray point sources in SFRs comprise pre-main sequence (PMS) stars as well as massive stars. Sometimes, X-ray emission from deeply embedded young stellar objects (YSO) is observed, albeit such observations remain rare (Pravdo et al. 2009). It is now firmly established that the shocked winds of young massive OB stars contribute to the heating of interstellar matter up to ≲10 MK (Townsley et al. 2003; Güdel et al. 2008). In older massive stellar aggregates, the combined action of stellar winds and supernova explosions results in powerful cluster winds and associated superbubbles (Chevalier & Clegg 1985). Higher temperatures (up to 100 MK) are observed in these objects. Hot, X-ray-emitting gas is present around massive stars and fills the large volumes of star clusters, and, in some cases beyond.

There is a small group of SFRs where hard, sometimes non-thermal X-ray emission is observed. In cases when strong fluorescent lines are seen in the spectra, the emission is explained by the presence of a recent supernova remnant (SNR) and its interaction with the cool dense material of a nearby molecular cloud (Takagi et al. 2002). However, in some prominent SFRs, such as RCW 38, the non-thermal X-ray emission cannot be easily explained unless the presence of magnetic fields is assumed (Wolk et al. 2002).

Magnetic fields, along with turbulence, play an important role in star formation (Crutcher et al. 2009). Magnetic fields were directly measured in M 17 (Brogan & Troland 2001) and Orion (Schleuning 1998), and are predicted to be a common feature in SFRs (Ferland 2009). If accelerated particles are present in the same volume, synchrotron emission would naturally occur.

A region within a few arcminutes of the OH maser ON 2 in Cygnus X is an established site of ongoing massive star formation. Following the literature we refer to this whole SFR as ON 2 (Dent et al. 1988; Shepherd et al. 1997). This region is located within the well-studied massive star cluster Berkeley 87.

One of the most interesting members of Berkeley 87 is the WO type star WR 142. Only three stars of this spectral type are known in the Galaxy, and the WO star in Berkeley 87 is the closest among them. Stars of this spectral type represent the evolutionary stage

immediately before the supernova or γ-ray burst explosion, and drive the fastest stellar winds among all stars. Berkeley 87 traditionally attracts the attention of high-energy astrophysics as a potential site of particle acceleration. Therefore, SFR ON 2 provides an ideal laboratory to study the interactions between an active star-forming region and the massive star feedback.

In this paper we present our *XMM-Newton* observations of the field encompassing ON 2 and Berkeley 87, and provide their analysis and interpretation. The paper is organized as follows. In Section 2 we introduce the SFR ON 2, and discuss its distance and relation to the star cluster Berkeley 87. The membership and evolution of Berkeley 87 is treated in Sect. 3. The analyses of *XMM-Newton* and *Spitzer* observations are presented in Sect. 4. In Sect. 5 we briefly address the distribution of point sources detected by *Spitzer*. In Sect. 6 we consider X-rays from massive stars in Berkeley 87. Section 7 is devoted to the X-ray emission from the H II region GAL 75.84+0.40. Section 8 concentrates on the observed properties of X-ray emission from ON 2S, the southern part of ON 2, while discussion on its origin is presented in Sect. 9. A comparison to other SFRs is presented in Sect. 10, and conclusions are drawn in Sect. 11. In the Appendix we briefly review the suggestions in the literature about the possible identification of γ-ray sources in Berkeley 87.

2. The massive star-forming region ON 2

Figure 1 shows the composite DSS optical and *Spitzer* IR image of SFR ON 2 and star cluster Berkeley 87. A large molecular cloud complex, Onsala 2C, observed in CO, is intimately associated with the whole ON 2 complex (Matthews et al. 1986). In a morphological model by Turner & Forbes (1982) based on studies of the reddening and obscuration, Berkeley 87 sits on the western edge of the heavily obscured SFR ON 2 and the associated giant molecular cloud Onsala 2C. Figure 2 gives a schematic representation of the morphology of the ON 2 region. The center of the massive star cluster Berkeley 87 is in the middle of the figure. The molecular cloud occupies the upper left quadrant. The sites of active star formation, as highlighted by compact H II regions, are located at the edges of a molecular cloud.

A *Spitzer* IRAC image of the region is shown in the right panel of Fig. 1. Following Dent et al. (1988) we will distinguish between northern and southern
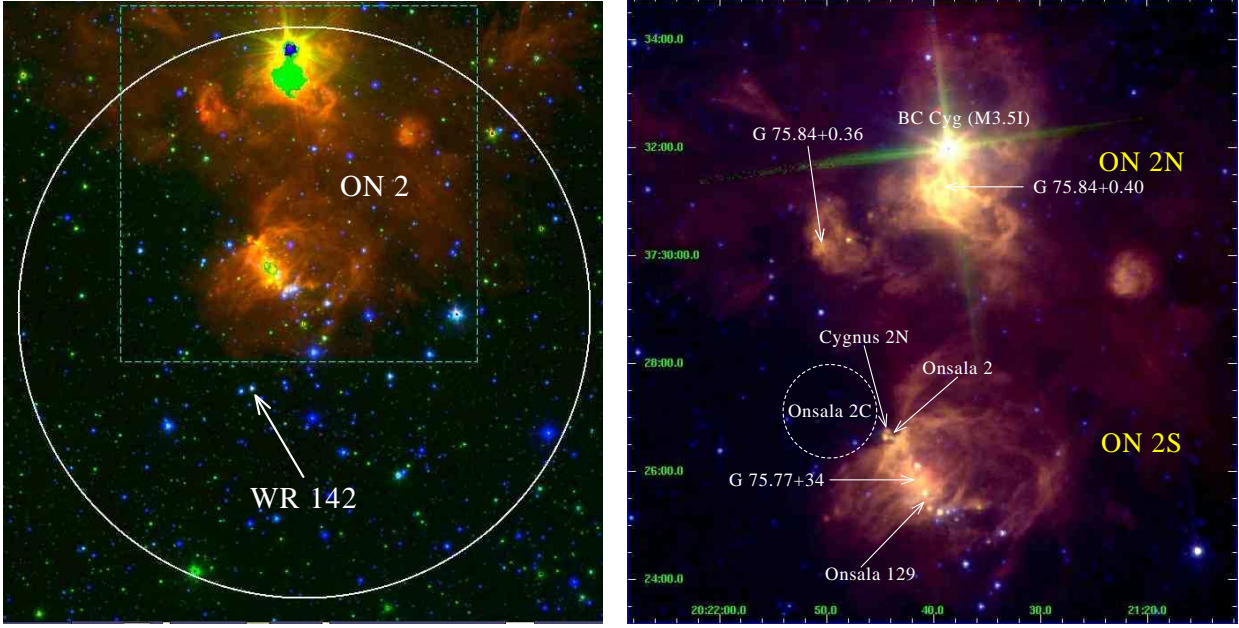
Fig. 1.— *Left panel*: Combined optical and IR image of Berkeley 87 and ON 2. The POSS2/blue image (Copyright Second Palomar Sky Survey 1993-1995 by the California Institute of Technology) is shown in blue, the *Spitzer* IRAC channel 1 (3.6 μm) is in green, and channel 4 (8 μm) in red. The large white circle represents the outer cluster boundary as determined from star counts by Turner & Forbes (1982). The center of the circle is at $20^h21^m37^s$, $+37°\,24'\,37''$ (J2000), the radius is 8′. The Berkeley 87 cluster is fully within the *XMM-Newton* field-of-view (30′). The approximate extend of the massive star-forming region ON 2 is shown by the dashed square. The region withing the square is enlarged in the right panel. *Right panel*: Combined IR *Spitzer* IRAC (3.6 μm blue, 4.5 μm green, 8.0 μm red) image of the massive star-forming region ON2. The H II regions described in the text are identified by arrows. The approximate location of the molecular cloud Onsala 2C is shown as a dashed circle. Image size is ≈12′×11′. North is up, and east is left.

H II regions, and introduce the notations ON 2N and ON 2S. The northern part, ON 2N, comprises the H II regions GAL 75.84+0.40 and GAL 75.84+0.36. ON 2S contains the H II regions Cygnus 2N (alias G75.78+0.34, Onsala 2N), Onsala 2 (alias [HLB98] Onsala 130), [L89b] 75.767+00.344, and [HLB98] Onsala 129 (Fig. 1). The UCH II regions Cygnus 2N and Onsala 2 are separated by only ≈ 2″.5 [1]. Onsala 2, Cygnus 2N, and Onsala 129 (Palagi et al. 1993; Hofner & Churchwell 1996; Shepherd et al. 1997).

Shepherd et al. (1997) studied ON 2S in molecular

lines and the 3 mm continuum. They detected three deeply embedded YSOs in Cygnus 2N, one of which is likely to be the driving engine of a molecular outflow. From the dynamical timescales of the outflows (∼30-50 kyr) and the high luminosities inferred for the YSOs (5000, 430, and 330 $L_\odot$) they suggest that a near-simultaneous massive star formation event occurred in this region ∼ 10^4 yr ago. This support similar conclusions made by Dent et al. (1988).

2.1. Distance to ON 2 and its relation to Berkeley 87

ON 2 is located in the Cygnus region, and thus we are looking tangentially to the Orion local spiral arm and observe numerous objects at different distances (Uyaniker et al. 2001). Reifenstein et al. (1970) estimate the distance to ON 2 as 5.5 kpc, while Turner & Forbes (1982) argue that ON 2 is located at the

---

[1]The Simbad data-base gives aliases of Onsala 2 as [WAM82] 075.77+0.34, OH 75.8+0.3, [HLB98] Onsala 130, and [PCC93] 414. The coordinates of Onsala 2 from Simbad are $20^h21^m43^s.8$, $+37°\,26'\,39''$ (J2000). However, the coordinates of [WAM82] 075.77+0.34 are $20^h21^m41^s.31$, $+37°\,25'\,53.5''$ (J2000) (Wink et al. 1982). This object is ≈54″ away from Onsala 2. The positional accuracy of Wink et al. (1982) is typically 5″. Therefore, [WAM82] 075.77+0.34 **is not** Onsala 2.
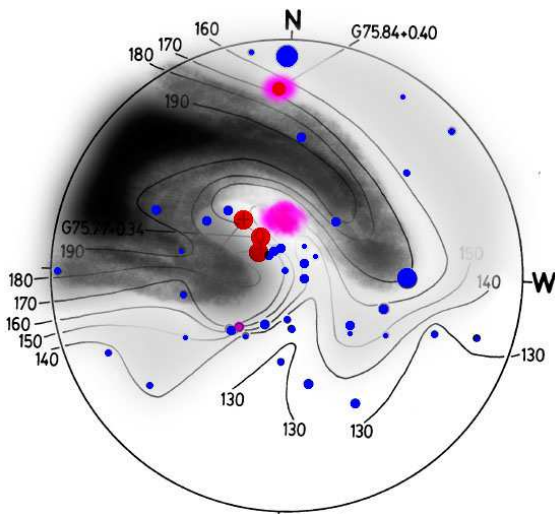
Fig. 2.— Sketch of the possible morphology of ON 2 based on Fig. 6 from Turner & Forbes (1982). The black circle is the same as in Fig. 1. The shaded area follows contour lines joining regions of similar space reddening (units of 0.01 mag in E_{B-V}). The pink elliptical regions represent approximately the patches of hard X-ray emission. The blue dots represent stars in Berkeley 87, the red spots represent UCH II regions. Not to scale.

same distance as the cluster Berkeley 87 and is physically connected with this cluster. Massey et al. (2001) obtained new photometric measurements of stars in Berkeley 87 and derived a distance of $d \approx 1600$ pc. Turner et al. (2006) augmented their previous studies of Berkeley 87 by a larger number of stars, and derived $d \approx 1230 \pm 40$ pc, which we adopt here.

Turner & Forbes (1982) notice that a trunk-like zone of heavy obscuration seen in Fig. 2 corresponds spatially with a CO clouds belonging to the Cygnus X complex. In a recent study Schneider et al. (2007) show that the UV radiation from the clusters within the Cygnus OB1 association, including Berkeley 87, affects the molecular cloud complex in the Cygnus X south region, and note that a distance between 1.1 and 1.3 kpc is favored from O stars spectroscopy. This supports the likely association between Berkeley 87 and ON 2.

3. The open star cluster Berkeley 87

Berkeley 87 is a relatively sparse, moderately reddened cluster, whose members represent some of the

key stages in the evolution of massive stars. The most intriguing is a WO-type star, WR 142. Analysis of its X-ray observations was presented in Oskinova et al. (2009). The brightest member of Berkeley 87, HD 229059, lies slightly off the cluster core. It is a binary system with a B1.5Iap and a lower-luminosity late-O or B0 star companion (Negueruela 2004). Mathys (1987) suggests that this star is a blue straggler. Close to the cluster center is the peculiar variable star V 439 Cyg. Negueruela (2004) identify this star as having B1.5Ve spectral type, while Massey et al. (2001) suggest a B[e] classification. The bright red supergiant BC Cyg of M3.5Ia type (Turner et al. 2006) is located at the north of the cluster, close to the H II region GAL 75.84+0.40. A possible spectroscopic binary BD+36°4032 (O8.5 V or O8.5III) (Negueruela 2004; Massey et al. 2001) is located immediately south of ON 2S.

The history of Berkeley 87 is not well understood. The ages of OB stars, the WO star, and the red supergiant star are in apparent disagreement with an evolution within a nearly coeval cluster.

Vanbeveren et al. (1998) found that 27% of the young Galactic massive clusters contain WR and red supergiant (RSG) members, and that such clusters must be older than 4 Myr. Moreover, WC/WO stars can co-exist with RSG stars only during a short time interval of $\sim$ a few $\times 10^5$ yr. Massey et al. (2001) studied Berkeley 87 among other Galactic open clusters. They suggested that OB stars in Berkeley 87 were formed within the time span of <1 Myr and are coeval with WR 142 at 3.2 Myr. Using evolutionary tracks of Schaller et al. (1992), they estimate the initial mass of WR 142 as $M_i = 70 M_\odot$. In the meantime, the initial mass of BC Cyg is $\lesssim 25 M_\odot$ (Levesque et al. 2005). A star of such mass must be older than 6.4 Myr when it reaches RSG stage (Schaller et al. 1992).

This apparent contradiction can be resolved with stellar evolutionary models that account for rotation (Meynet & Maeder 2005). We have recently found indications that WR 142 may be a fast rotator (Oskinova et al. 2009). In fast rotating stars, the RSG stage will occur earlier, perhaps even during the H-burning stage, while the WO stage occurs later compared to the non-rotating models. Therefore, the simultaneous presence of a RSG and a WO star can be explained if Berkeley 87 is $\sim$ 4-6 Myr old.

Assuming that the most massive star in Berkeley 87 has an initial mass higher than $80 M_\odot$ and the universal initial mass function (IMF), we estimate that about
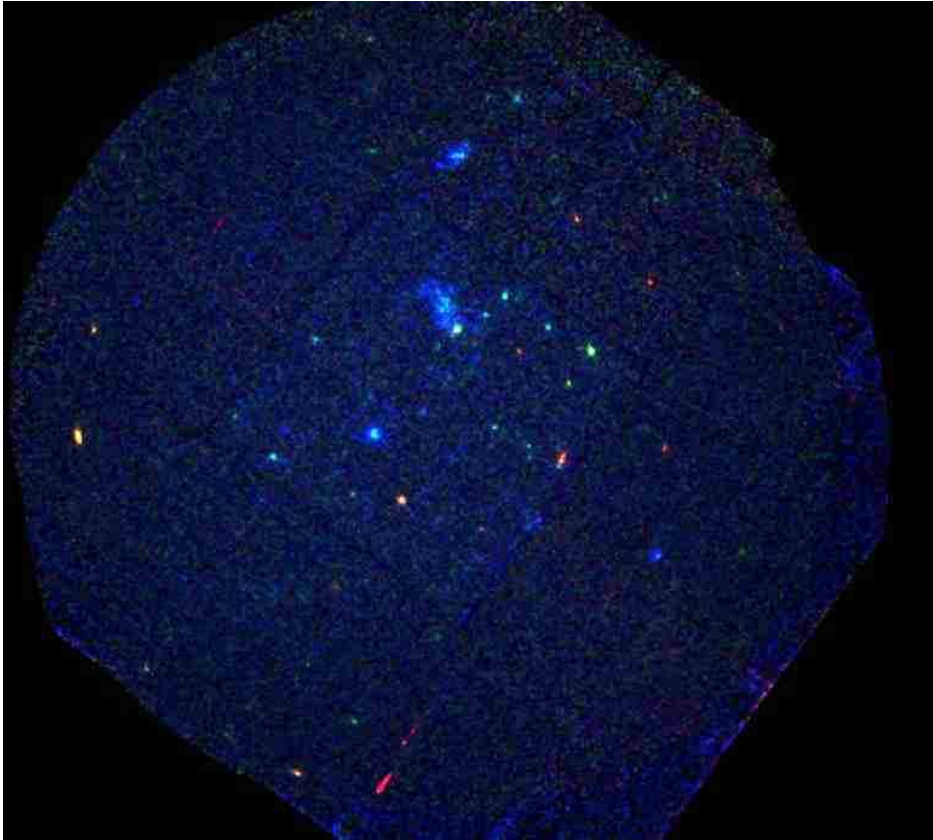
Fig. 3.— Combined *XMM-Newton* MOS1, MOS2, and PN image of the Berkeley 87 in the 0.25 to 12.0 keV band (red=0.25-1.0 keV, green=1.0-2.5 keV, blue=2.5-12.0 keV). Image size is $\approx 30' \times 30'$. North is up, and east is left.

30 stars with initial mass more than $10\,M_\odot$ should be present in Berkeley 87. This estimate is consistent with the 22 known massive stars in Berkeley 87 given the uncertainties (Massey et al. 2001). In this case, the total mass of Berkeley 87 should be $\approx 1200\,M_\odot$. The number of low mass stars with masses between $0.5\,M_\odot$ and $3\,M_\odot$ can be estimated as ≈ 2000.

4. *XMM-Newton* and *Spitzer* observations of Berkeley 87.

Berkeley 87 was observed by *XMM-Newton* during two consecutive satellite orbits [2]. The data were merged and analyzed using the software sas 8.0.0. After the high-background time intervals have been rejected, the combined exposure time of all detectors was ≈ 100 ks. We followed the standard procedure for the source detection, setting the minimum detec-

tion likelihood to 5. That yielded the detection of 130 point sources as well as two regions of diffuse X-ray emission.

A combined EPIC MOS1, MOS2, and PN image of Berkeley 87 and its surroundings is shown in Fig. 3. Two prominent hard (blue color) extended X-ray sources are located in the ON 2 SFR, slightly off to the north from the image center. The combined X-ray and IR images of ON 2 are shown in Fig. 4. The extended X-ray emission traces the eastern edge of ON 2S region and is also observed from the H II region G75.84+0.40 in ON 2N.

The angular resolution of *XMM-Newton* is $\lesssim 6''$. To exclude the potential confusion of extended emission with an unresolved stellar point source, we inspected optical and infrared images with higher angular resolution. The region around the Berkeley 87 cluster has been partially imaged in the mid-IR with the *Spitzer* InfraRed Array Camera (IRAC; Fazio et al. 2004) with
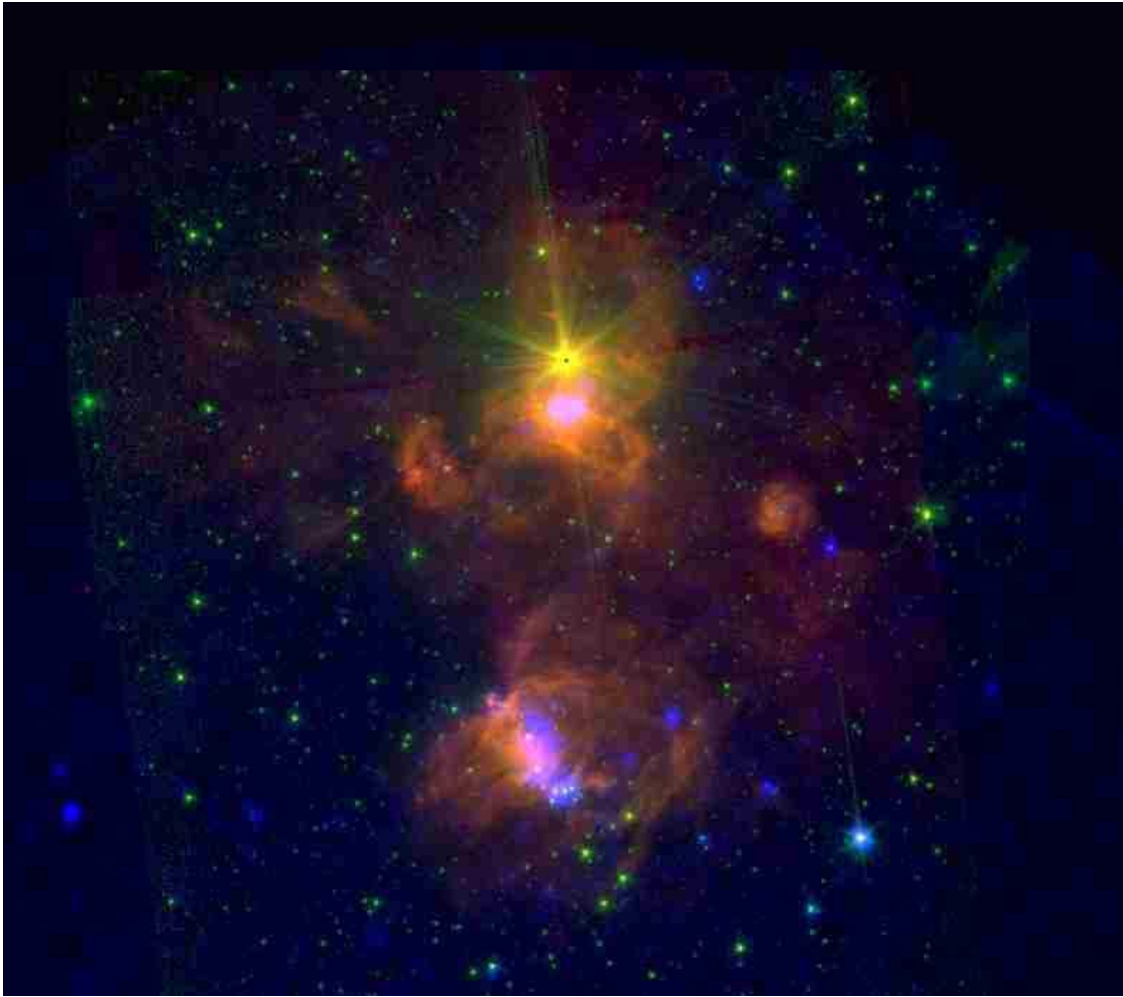
---

[2]ObsId 0550220101, ObsId 0550220201

Fig. 4.— Image of ON 2 combined from *XMM-Newton* EPIC (0.25 to 12.0 keV band, blue) and *Spitzer* IRAC (3.6 μm, green, and 8.0 μm, red).

angular resolution of ≲2″. The northern half of Berkeley 87, including the H II regions GAL 75.84+0.40 and GAL 75.78+0.34, has observations in all four IRAC bands (3.6, 4.5, 5.8 and 8.0 μm) but the southern half of Berkeley 87 is only covered in 3.6 and 5.8 μm images. We downloaded all applicable IRAC observations from the *Spitzer* archive and combined the basic calibrated data to form mosaic images of the entire region using the MOPEX software package. More information on the instruments and pipeline processing can be found at the *Spitzer* Science Center's Observer Support website[3].

5. Brief analysis of distribution of IR sources in Berkeley 87.

YSOs can be identified by their IR excess, since they are still surrounded by dusty disks and envelopes that absorb stellar light and radiate at IR wavelengths. Theoretical predictions regarding the location of YSOs in color-magnitude diagrams (CMDs) and color-color diagrams (CCDs) can be used to compare with observations in order to study the YSOs. Based on *Spitzer* IRAC and MIPS observations, this method was recently used by Gruendl & Chu (2009) to search for YSOs in the Large Magellanic Cloud. We use a similar method to search for objects with near- and mid-infrared excess in Berkeley 87.
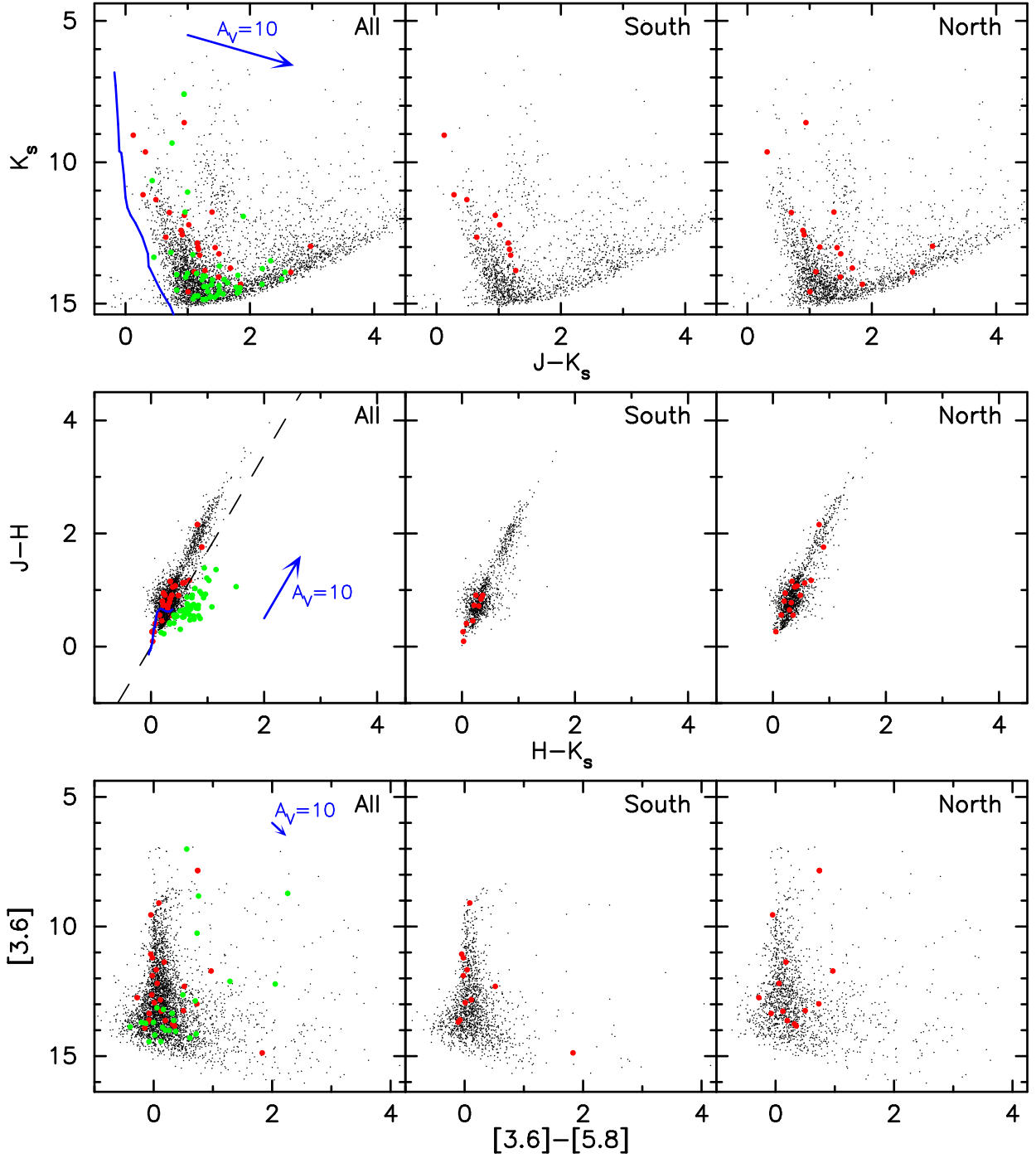
Fig. 5.— CMDs and CCD based on IRAC and 2MASS photometry. The panels marked "all" use the photometric data for the entire field, while the panels marked "south" use a subset which exclude the ON 2 SFR, and the panels marked "north" correspond to the ON 2 SFR. In the leftmost panels of each row the arrow indicates the reddenning vector expected for A_V=10 (Cardelli et al. 1989) and the solid lines in in the K_s versus $J - K_s$ CMD and $J - H$ versus $H - K_s$ CCD correspond to the expected location of the zero-age main sequence for an assumed distance of 1.23 kpc (Bessell & Brett 1988). Objects plotted with a filled red circle have a possible X-ray point source counterpart. Objects plotted with green circles are more than 1-σ beyond the black dashed line ($J - H = 1.692H - K$) indicating possible excess infrared emission (Allen et al. 2004).
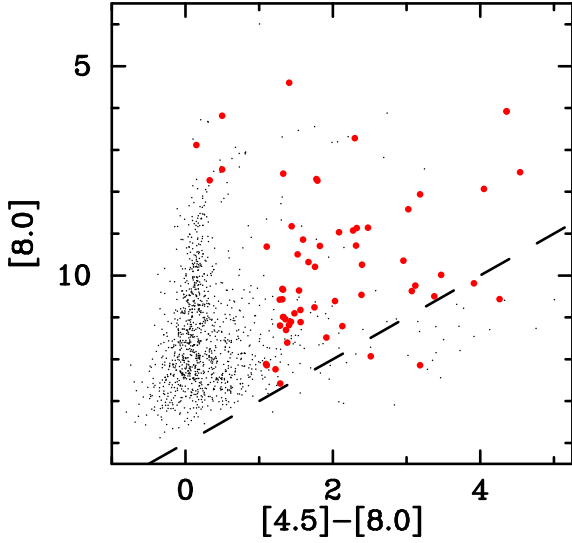
7

Fig. 6.— An [8.0] versus [4.5]−[8.0] CMD showing all sources in the Berkeley 87 region. Red points indicate sources from Figure 5 with [3.6]-[5.8]>1.0. Background galaxies and AGN should generally fall below the dashed line, [8.0]=14−([4.5]−[8.0] (Harvey et al. 2006).
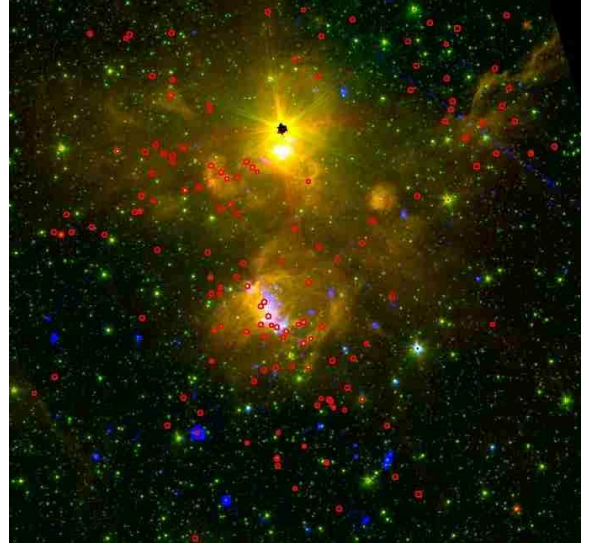

Fig. 7.— Combined *Spitzer* IRAC (3.6 μm green, 4.5 μm red) and *XMM-Newton* EPIC (blue) image of Berkeley 87. The red regions mark the positions of IRAC sources with [3.6]−[5.8]>1.0 which may be YSOs. Image size is ≈22′×20′. North is up, and east is left.

Aperture photometry was performed on the 3.6, 4.5, 5.8, and 8.0 μm IRAC images to obtain mid-IR flux densities for sources throughout the Berkeley 87 region. The results at each wavelength were combined for sources with <1″5 positional coincidence. We also obtained near-IR (JHK_s) flux densities from the Two Micron All Sky Survey Point Source Catalog (2MASS PSC; Skrutskie et al. 2006) and combined these with the mid-IR measurements, again requiring a <1″5 positional coincidence for a positive match between sources detected in different bands.

The resulting catalog does not have complete spatial coverage at all wavelengths over the entire region discussed in this paper. Specifically there are no IRAC observations at 4.5 and 8.0 μm for declinations south of +37°20′ (the southern and unobscured half of Berkeley 87). Therefore to search for evidence for a population of YSOs and PMSs we have confined ourselves to using the 2MASS JHK_s bands and the IRAC 3.6 and 5.8 μm bands. In Fig. 5 we present color-color and color-magnitude diagrams (CCDs and CMDs) that illustrate the difference in the stellar population we see when we compare: (1) the entire Berkeley 87 region, (2) the southern, unobscured, portion of Berkeley 87 and (3) the northern portion of Berkeley 87 which

contains the SFR ON 2. Specifically the sources for the entire Berkeley 87 region are within a box centered at RA=20^{h}21^{m}37^{s}7, DEC=+37° 24′ 43″5, with ΔRA=20′, ΔDEC=20′, while the southern region is defined by a box centered at RA=20^{h}21^{m}37^{s}7, DEC=+37° 17′ 22″5, with ΔRA=20′, ΔDEC=10′, (i.e. excluding the ON 2 SFR), and the northern region is defined by a box centered at RA=20^{h}21^{m}37^{s}7, DEC=+37° 28′ 28″4, with ΔRA=20′, ΔDEC=12′, (i.e. the ON 2 SFR and surroundings). While the near-IR CCDs and CMDs constructed from 2MASS data appear similar in the north and south, the [3.6] versus [3.6]-[5.8] CMD, constructed from the IRAC observations, reveal a higher density of sources with red mid-IR colors (excess mid-IR emission). After correcting for the area we find that for [3.6]-[5.8]>1.0 there are ~4 times as many red sources in the northern region than in the south (see lower panel in Fig. 5).

The lack of MIPS 24 μm observations over much of the region, the incomplete IRAC coverage, and the limited sensitivity of 2MASS prevent a more detailed assessment as to the true nature of these red sources. Nevertheless, we speculate that these are YSOs associated with Berkeley 87. For instance, if we select from the $J − H$ versus $H − K_s$ CCD those 2MASS sources
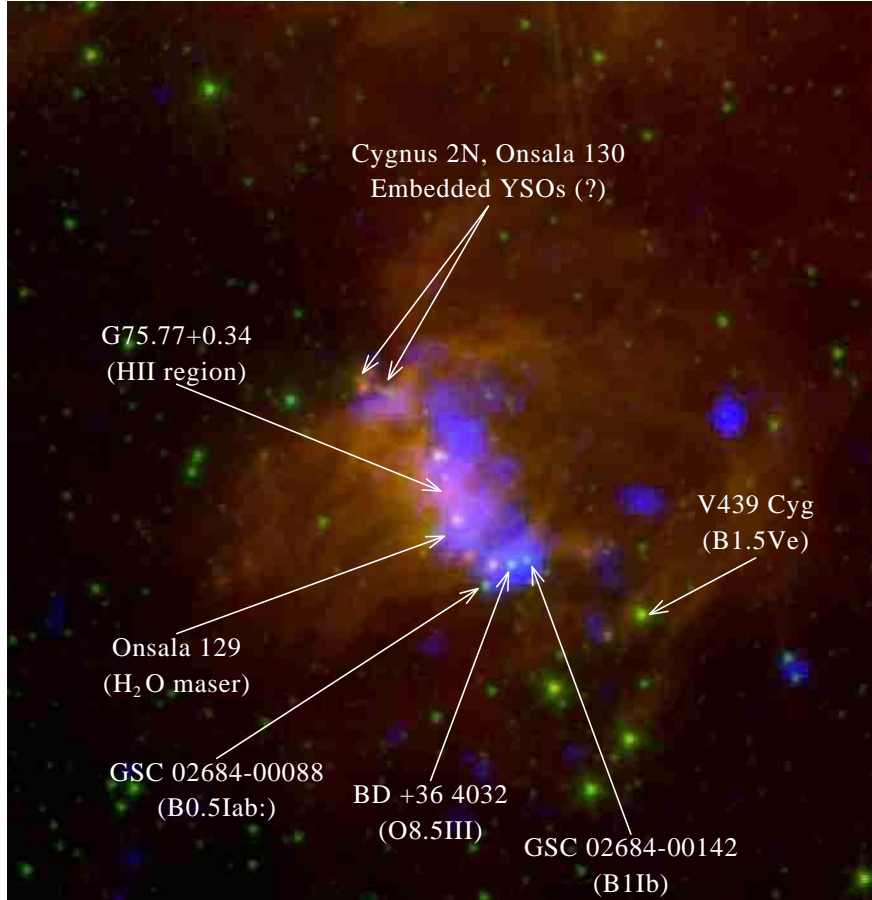
Fig. 8.— Combined *XMM-Newton* MOS2 (0.25 to 12.0 keV band, blue) and *Spitzer* IRAC (3.6 μm, green, and 8.0 μm, red) image of ON 2S. The image size is $\approx 6.5' \times 6.5'$.

with near-IR execss, we find 49 sources (green circles in the middle panel of Fig.5). Only three of these objects with near-IR excess are among the sources with mid-IR excess identified in the [3.6] versus [3.6]-[5.8] CMD. Thus most of the sources with mid-IR excess escape detection with 2MASS.

We can, however, rule out that the sources with [3.6]-[5.8]>1.0 are dominated by background galaxies. In Fig. 6 we present a [8.0] vs. [4.5]−[8.0] CMD for all sources with available data and find that most of them lie above the cutoff that has been used to separate background galaxies and AGN in other population studies (Harvey et al. 2006; Kozłowski & Kochanek 2009). Hence we believe that there are strong indications that the IRAC sources in Berkeley 87 with mid-IR excess are dominated by YSOs. In order to confirm and better quantify the YSO population throughout

this region, deeper near-IR and more complete mid-IR observations are required.

To better illustrate the distribution of these candidate YSOs in ON 2 we plot the locations of all sources with [3.6]-[5.8]>1.0 in Fig. 7. We have also searched for possible X-ray counterparts to the 2MASS and IRAC points sources by comparing their positions and requiring a coincidence better than 3″ for a positive match. A total of 47 matches were found but only one of those matches had a significant mid-IR excess (see Fig. 5). The near-IR fluxes and colors of nearly all the sources with possible X-ray counterparts are consistent with normal main sequence stars.

The very low X-ray detection rate of young stars in Berkeley 87 is not surprising. The limiting sensitivity of our *XMM-Newton* observations is $F_X \approx 1 \times 10^{-14}$ erg s^{-1} cm^{-2}. Taking into account the aver-

9

Table 1: The OB type stars detected by *XMM-Newton* and their parameters

Star	RA (J2000)	DEC (J2000)	Sp.type	$\log \frac{L_{bol}}{L_\odot}$	$N_H [10^{21} \text{ cm}^{-2}]$	$\log \frac{L_X}{L_{bol}}$
HDE 229059	$20^h 21^m 15^s.37$	$37° 24' 31.3''$	B1Ia	5.6	8.6	-7.5
Berkeley 87-4	$20^h 21^m 19^s.25$	$37° 23' 24.3''$	B0.2III	4.7	7.4	-7.1
BD +36°4032	$20^h 21^m 38^s.67$	$37° 25' 15.5''$	O8.5III	5.1	7.8	-7.3

age absorbing column in the direction of Berkeley 87, $N_H \approx 8 \times 10^{21} \text{ cm}^{-2}$, the unabsorbed flux for a thermal source of X-ray emission with $kT_X = 0.8 \text{ keV}$ is $F_X \approx 9 \times 10^{-14} \text{ erg s}^{-1} \text{ cm}^{-2}$. At the 1.23 kpc, this corresponds to $L_X \approx 2 \times 10^{31} \text{ erg s}^{-1}$. Studies of low-mass stars in the Orion Nebular Cluster shown that there is a correlation between stellar age, mass, and X-ray activity (Flaccomio et al. 2003). The X-ray luminosities of a few Myr old low- and solar-mass PMSs are lower than the detection limit of our observations.

The CMDs shown in Fig. 5 provide one more indirect evidence that the SFR ON 2 and star cluster Berkeley 87 are located at the same distance. The magnitudes of sources located in the ON 2 region do not differ significantly from the magnitudes of sources in southern part of Berkeley 87. If ON 2 were 4 times more distant than Berkeley 87 (see discussion in Section 2.1), one would expect many more faint sources in the right panels in Fig. 5. The spatial distribution of YSOs across the entire ON 2N (Fig. 7) confirms earlier suggestions of Turner & Forbes (1982) and Dent et al. (1988) that star formation occurred nearly simultaneously over this whole SFR.

6. X-ray emission from massive stars in Berkeley 87.

In general, all massive stars with spectral types earlier than B1.5 are X-ray emitters. Turner & Forbes (1982) identified 17 stars in Berkeley 87 as having early OB spectral types. Among them only three were unambiguously detected in our *XMM-Newton* observation. This is because the large interstellar extinction in the direction of Berkeley 87 hampers the detection of soft X-ray sources such as OB stars.

A combined X-ray and IR images of ON 2 and ON 2S are shown in Figs. 4 and 8. The O-type giant BD +36°4032 (Berkeley 87-25) is located at the southern tip of the ON 2S. Neighboring it are two B-type stars, separated by $8''$ and $15''.6$ from BD +36°4032. Among these only the O star is detected.

All spectra in this paper were analyzed using the

XSPEC software (Arnaud 1996).

The X-ray spectrum of BD +36°4032 can be fitted with a thermal plasma model (*apec*) with temperature $kT_X = 0.6 \pm 0.1 \text{ keV}$, and a neutral hydrogen absorption column $N_H = (8 \pm 1) \times 10^{21} \text{ cm}^{-2}$. The unabsorbed model flux is $F_X \approx 2 \times 10^{-13} \text{ erg cm}^{-2} \text{ s}^{-1}$, corresponding to $L_X \approx 4 \times 10^{31} \text{ erg s}^{-1}$. This is the X-ray brightest massive star in Berkeley 87.

Two B-type stars, HDE 229059 (Berkeley 87-3) and Berkeley 87-4, are also detected in our observation. Their X-ray spectra are fitted using a thermal plasma model with $kT_X = 0.6 \pm 0.2 \text{ keV}$ corrected for interstellar column $N_H = (8 \pm 1) \times 10^{21} \text{ cm}^{-2}$.

We use the *UBV* photometry and spectral types determined in Turner & Forbes (1982) to derive stellar bolometric luminosities and color excesses E_{B-V}. The neutral hydrogen column densities are then estimated using $N_H = 5.0 \times 10^{21} E_{B-V}$ H-atoms cm^{-2} (Bohlin & Savage 1981) and listed in Table 1 for the stars that are detected by *XMM-Newton*. The absorption columns inferred from the analysis of the X-ray spectra are in good agreement with those from *UBV* photometry.

The ratio of X-ray and bolometric luminosities for the detected OB stars (see Table 1) appear to be slightly lower than the typical value of 10^{-7} for OB stars (e.g. Oskinova 2005). This is because the soft X-rays are missing due to the large interstellar absorption. Our crude one-temperature spectral models fitted to the observed spectra underestimate the contribution from the soft spectral range. Bearing this in mind, the level of X-ray emission from the OB stars in Berkeley 87 appears to be normal for stars of these spectral types.

7. X-ray emission from the H II region GAL 75.84+0.40 in ON 2N

In this section we will address the H II regions in the northern part of ON 2 (see Fig. 1). While no X-ray emission is detected from GAL 75.84+0.36, GAL 75.84+0.40 is a spectacular source of diffuse X-rays. We consider it in detail below.
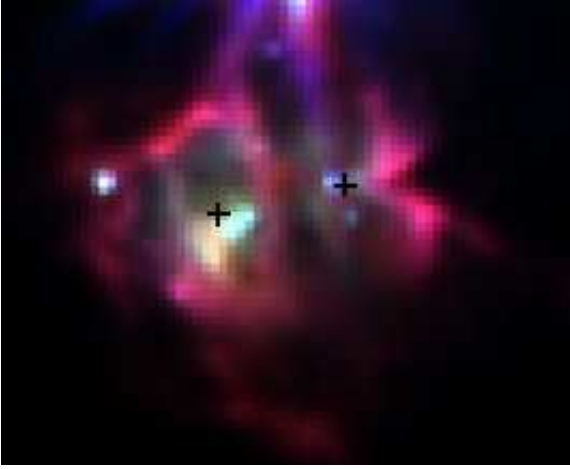
Fig. 9.— Zoomed ON 2N region from combined *Spitzer* IRAC 3.6, 4.5, and 8.0 μm image are shown as red, green and blue, respectively. Crosses mark the positions of source A (to the west) and source B (to the east). The image size is ~1'.5×1'.2 with north up and east to the left.

7.1. Morphology of H II region GAL 75.84+0.40

Matthews et al. (1973) conducted a radio survey of ON 2. They noticed that GAL 75.84+0.40 has a complex morphology, and suggested that it consists of two compact H II regions – the first is GAL 75.84+0.40 A to the east, and the second is GAL 75.84+0.40 B to the west. Within each compact H II region, there exists a corresponding point source in the 2MASS PSC. These two IR point sources are separated by ≈14'.'3 (or 0.09 pc at d=1.23 kpc). Their coordinates and K_s magnitudes are given in Table 2. Corresponding sources at these positions can be also seen in the *Spitzer* images (see Fig. 9).

In the IRAC bands source A has flux densities of 52.1±3.7 mJy and 44.1±5.0 mJy at 3.6 and 4.5 μm, respectively ([3.6]≃9.32 mag and [4.5]≃9.02 mag), which are also consistent with an embedded O5-6V type star. On the other hand, for source B, we found a flux density of 194.2±7.3 mJy at 4.5 μm ([4.5]≃7.4)

Table 2: 2MASS point sources in GAL 75.84+0.40

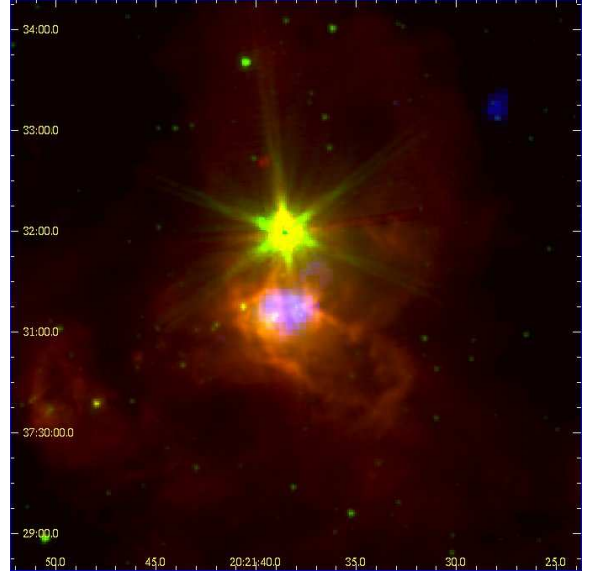|	RA (J2000)	DEC (J2000)	m_K
A	20^{h}21^{m}37^s.98	+37° 31' 15.23''	9.628
B	20^{h}21^{m}39^s.07	+37° 31' 09.27''	9.665

Fig. 10.— Combined *XMM-Newton* MOS2 (blue) and *Spitzer* IRAC 3.6 μm (green) and 8.0 μm (red) images of ON 2N. The image size is ~ 5'.5 × 5'.5 with north up and east to the left.

which suggests a mid-IR excess if the 2MASS *K*-band source corresponds to a early type star. Inspection of the 2MASS and IRAC images for sources A and B reveal that both are amid complex diffuse emission but that while source A appears to be a single point source, source B appears elongated at all bands. We suggest that source B may be either a multiple or its flux measurements may suffer significant contamination from the surrounding diffuse emission.

Garay et al. (1993) presented an alternative to Matthews et al. (1973) view on the morphology of GAL 75.84+0.40. Based on VLA radio maps they was suggested that GAL 75.84+0.40 is an inhomogeneous shell of gas with outer radius ~ 17'', ionized by a single O-type central star. The highest resolution VLA 2 cm radio continuum maps show the two component structure which can correspond to the bright rims of the shell. The "two" compact H II regions suggested by Matthews et al. (1973) can be the brightest parts of this shell. Similar shell morphology, with brighten rims has been seen in planetary nebulae, post-AGB stars, and supernova remnants.

11

Fig. 11.— The same as in Fig. 9 but with contours of X-ray emission (contours are spaced logarithmically).

7.2. X-ray emission from GAL 75.84+0.40

A combined X-ray and IR image of the northern part of ON 2 is shown in Fig. 10, while Fig. 11 displays the IR *Spitzer* image overlaid with contours of the X-ray emission. The latter is extended and fills a nearly circular region centered at 20^h21^m38, $+37°\,31'\,14''$ (J2000), slightly offset from the 2MASS source "B" (Table 2). The source detection task indicates that the X-rays are diffuse.

The extracted spectrum of the diffuse X-ray emission in GAL 75.84+0.40 is shown in Fig. 12. The Cash statistics was used to fit the spectrum by both thermal and by power-law models. The spectrum has a relatively low signal-to-noise ratio and can be equally well fitted either by thermal or by non-thermal emission. The best fit parameters are included in Table 4. The spectrum is heavily absorbed. The absorbing column is $N_H \approx 4.5 \times 10^{22}\,\mathrm{cm}^{-2}$, corresponding to $E_{B-V} \approx 9$.

Turner & Forbes (1982) determine from optical the interstellar absorption in the direction of GAL 75.84+0.40 as E_{B-V}=1.7. Using $N_H = 5.0 \times 10^{21} E_{B-V}\,\mathrm{cm}^{-2}$, the column density is $N_H = 8.5 \times 10^{21}\,\mathrm{cm}^{-2}$, i.e. a factor of five smaller than inferred from the X-ray spectral fits. Thus, we observe X-ray emission from one or more deeply embedded sources.
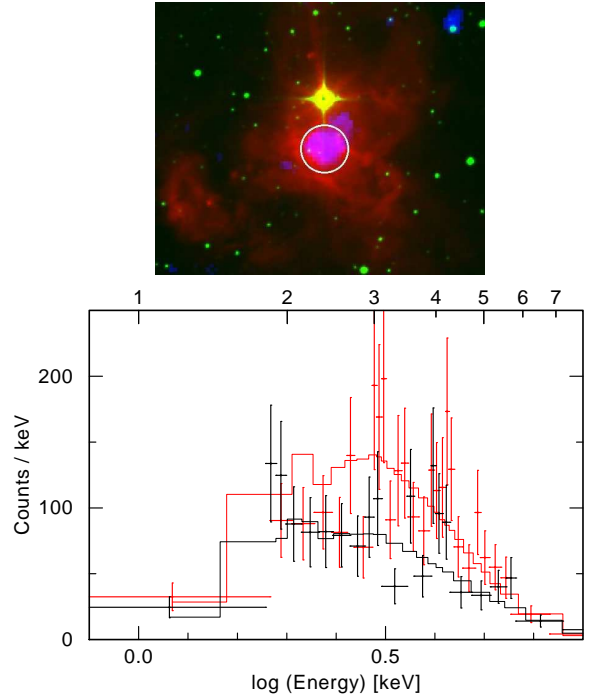

Fig. 12.— *Upper panel*: Same as in Fig. 10. The white circle shows the spectrum extraction region. *Lower panel*: The PN (red) and MOS2 (black) spectra of GAL 75.84+0.40. The best fit thermal plasma models plotted as solid lines for the corresponding detectors. The parameters of the model are given in Table 4.

7.3. Discussion on the Origin of the X-ray Emission from GAL 75.84+0.40

The ionizing stars of H II regions are intrinsic sources of X-ray emission. Assuming that stars GAL 75.84+0.40 contribute to the observed X-ray emission, we can obtain constraints on their stellar type. From the X-ray spectroscopy we determined $E_{B-V} \approx 9$. Adopting $R_V = 3.1$, one obtains $A_V = R_V E_{B-V} \approx 28$ mag. The ratio between visual and K-band extinction is $A_V/A_K = 8.9$ (Moneti et al. 2001). From the 2MASS Catalog, both stars in GAL 75.84+0.40 have $m_K \approx 9.6$ mag, corresponding to $M_K = -4$. Comparing with PoWR stellar atmosphere models (Hamann & Gräfener 2004), this K-band absolute magnitude corresponds to roughly an O5 type star.

A number of earlier estimates for the ionizing source of GAL 75.84+0.40 exist. For example, Dent et al. (1988) used the far-infrared flux to derive the

12

Table 3: Decomposing extended region filled with X-ray emission in ON 2S[a]

Region (as in Fig 13)	RA (J2000)	DEC (J2000)	Emission	Origin
OB	20^h21^m38	$+37°\,25'\,15''$	thermal stellar wind	OB stars
H	20^h21^m40	$+37°\,25'\,34''$	?	star? UCH II ?
CN	20^h21^m43	$+37°\,26'\,33''$	?	AGN? UCH II ?, star?
R	20^h21^m41	$+37°\,26'\,07''$	?	star? UCH II ?
D	20^h21^m41	$+37°\,26'\,35''$	non-thermal?	magnetic field? YSOs?

[a] coordinates of the centers of the regions

spectral type of the ionizing star in GAL 75.84+0.40 to be later that O9.7 assuming a distance of 1 kpc. In contrast, Matthews et al. (1973) found that two O8V stars were needed to account for the radio continuum measurements of the H II region after adopting a distance of 5.5 kpc. Finally, Garay et al. (1993) determined that a single O6V star could explain their radio continuum measurements after assuming a distance of 4.1 kpc. The only way to reconcile these earlier results with the O5 spectral type derived from the 2MASS magnitudes and X-ray spectroscopy is to assume that the X-ray source is embedded deeper than the ionizing stars. Note that this conclusion is independent of the adopted distance.

Thus, there are good arguments that the ionizing stars in GAL 75.84+0.40 are not the main source of the observed X-ray emission: the X-ray source is deeper embedded, extended, and hard or non-thermal.

The X-rays in GAL 75.84+0.40 fill a nearly circular area, with no obvious IR source being correlated with its center (see Fig 11). One of the possibilities to explain this can be an embedded cluster of young stars behind the H II region, which we observe in projection, and which is the source of X-ray emission. However, given the small linear extension of the X-ray source (0.1 pc) and the character of its spectrum, a cluster of pre-main sequence stars seems to be an unlikely explanation. Albeit some contribution from point sources is possible, we believe that a truely diffuse component is present in GAL 75.84+0.40.

Only a handful of star-forming regions with similar properties of X-ray emission is presently known (see Table 5). Besides the neighboring region ON 2S which we discuss in the next section, hard diffuse emission on similar spatial scales is observed in the massive SFR RCW 38 (Wolk et al. 2002). An old shell-type SNR was considered as a possible explanation. However, this explanation seems implausible in the case of GAL 75.84+0.40. Similar to the conclusions by Wolk
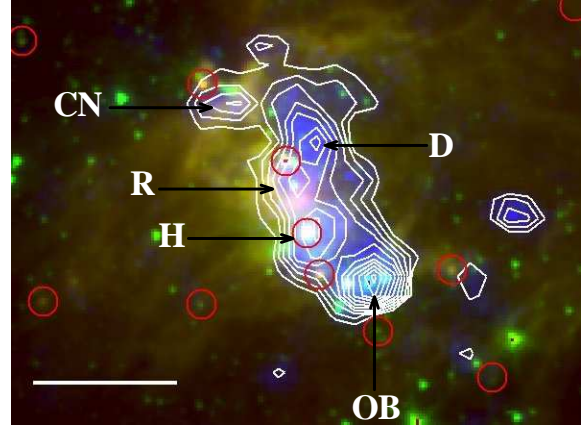

Fig. 13.— The same as in Fig. 8, but with over-plotted contours (log scale) of X-ray emission. The red circles are around young stars identified from *Spitzer* photometry. The regions discussed in the text are identified by letters and arrows. The white bar in the low left corner has 1′ length.

et al. (2002) we suggest that invoking magnetic fields in the SFR may be required to understand their hard X-ray emission. We will return to this point when discussing the X-rays from ON 2S in Sect. 8.

8. The ON 2S region

In this and the following section we consider the southern ON 2S region (Fig. 1) and the X-ray emission detected in its vicinity. Fig. 8 shows combined X-ray and IR images of ON 2S. In striking contrast to ON 2N, the extended X-ray emission in ON 2S does not coincide spatially with the UCH II regions and maser sources. Instead, the extended X-ray emission is observed to the east of the photo-dissociation region traced by the *Spitzer* images.

The ON 2S region is complex and compact, and

13

our *XMM-Newton* data are unable to fully resolve the individual components of the extended region. Nevertheless, the $\lesssim 4.5''$ angular resolution of the MOS2 camera allows an investigation of the morphology of the hot gas. Figure 13 displays the combined *Spitzer* and *XMM-Newton* image overlaid with contours of X-ray emission. We distinguish five X-ray sources in ON 2S, corresponding to the local maxima in the contours. The coordinates of these sources are given in Table 3. The regions designated "CN", "R", "H", and "OB" were detected as point sources by the source detection software. The region "D" is detected as a diffuse source. In the following, we first analyze the point-sources, and then the diffuse X-ray emission.

8.1. X-ray emission from point sources in ON 2S.

Faint X-ray emission is detected south from Cygnus 2N (region marked CN in Fig. 13). Albeit this emission appears extended in the adaptively smoothed image, the source detection software finds a point source at this location, coinciding within $0\rlap{.}''7$ with the faint star USNO-B1.0 1274-0505781 (B1=18.08 mag). No point source is detected at this position in any of the *Spitzer* IRAC channels. Similarly, no continuum radio source at this position was found by Shepherd et al. (1997).

The X-ray emission from the point source in CN is heavily absorbed, $N_{\rm H}\gtrsim 2\times 10^{22}\,{\rm cm}^{-2}$, and hard (see spectrum in panel 3 in Fig. 14). The absorbed flux is $F_{\rm X}=(3.0\pm 1.3)\times 10^{-14}\,{\rm erg\,cm}^{-2}\,{\rm s}^{-1}$. Because of its high absorption we exclude that the source is a foreground star. It could be either an embedded young star, or a background object (a Galactic star or an AGN). We consider the latter possibility as more likely, due to the lack of *Spitzer* or radio counterparts. However, on the basis of *XMM-Newton* observations we cannot rule out the interesting possibility that the X-ray emission south of Cygnus 2N originates from diffuse gas, while the close coincidence with a faint star is accidental.

The region "R" is $\approx 8''$ away from the radio source GRS 75.77+0.34, and $\approx 6''$ away from a young star we identified from *Spitzer* images. It is plausible, that the radio source and the young star are, in fact, one object. It is also plausible to assume that the observed X-rays, at least partly, are associated with the star. It is interesting to note that a very red object seen only at 8μm in *Spitzer* images is located in the area R.

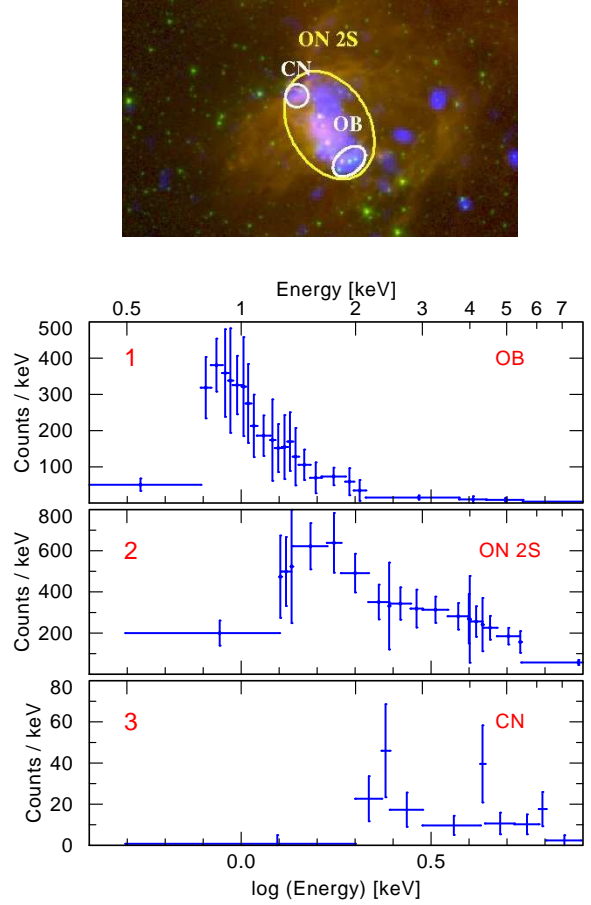The X-ray source in the region "H" (see Fig. 13) is located some $10''$ away from the Maser 075.76+00.34

Fig. 14.— *Upper panel*: Same as in Fig. 8. The spectrum extraction regions are shown. *Lower panel*: *XMM-Newton* PN spectra of three regions in ON 2S. The spectrum of the are containing OB-type stars is shown in plot 1. The spectrum of whole ON 2S is shown in plot 2. The spectrum of region close to Cyg 2N is shown in plot 3.

(Hofner & Churchwell 1996), and $6''$ away from the optical star Berkeley 87-83. The X-ray emission from H is too faint to constrain its morphology, and to extract useful spectral information. Hence the nature of the X-ray emission from this area remains unclear. It could be due to unresolved young star(s) or a diffuse source.

The X-ray emission from the region "OB" is dominated by O star BD $+36°4032$, and was discussed in Sect. 6.

In Fig. 14 we compare the spectra extracted from the whole ON 2S region and from the smaller areas
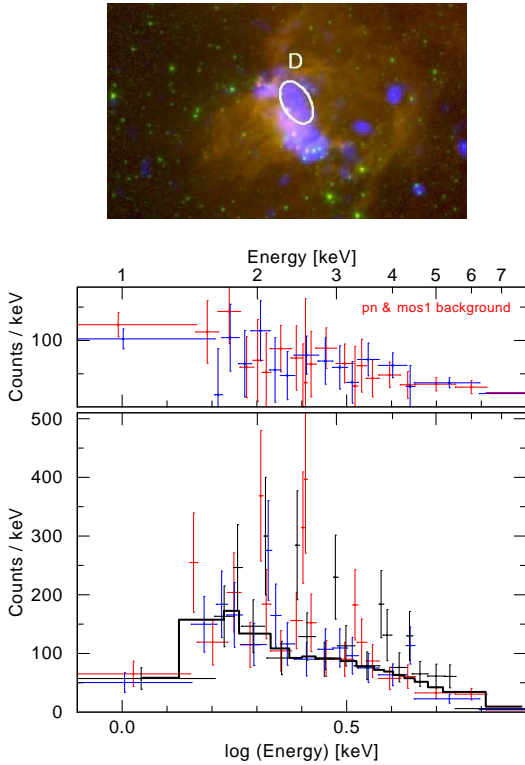
Fig. 15.— *Upper panel*: Same as in Fig. 8. The spectrum extraction region is shown. *Lower panel*: The background spectra are shown in the upper plot. *XMM-Newton* PN, MOS1 and 2 spectra of diffuse emission in the region D are shown in the lower plot. The MOS2 best fit model is shown as solid line, parameters of the models are given in Table 4.

"CN" and "OB". It is apparent that the spectrum of the OB region is much less affected by absorption. The spectrum extracted from the large area is strongly absorbed and quite hard, showing that hard X-ray emission from embedded sources dominates the whole ON 2S region.

8.2. Extended hard X-ray emission from ON 2S.

In the *XMM-Newton* images the X-ray emission from the region "D" in Fig. 15 appears to be truely diffuse. We cannot fully exclude the presence of discrete sources embedded in the diffuse emission, albeit we did not find any such sources in the available multiwavelength catalogs, radio, IR and X-rays images. From analysis of the *XMM-Newton* images, we estimate that the diffuse X-ray emission occupies

$\approx 3200\, \mathrm{arcsec}^2$. At a distance of $1.23\,\mathrm{kpc}$ this corresponds to $\approx 0.16\,\mathrm{pc}^2$ ($2.25\,\mathrm{pc}^2$ at a distance of $5.5\,\mathrm{kpc}$ respectively).

The spectrum of diffuse emission is shown in Fig. 15. The inferred absorption column density strongly exceeds the one found in the direction of neighboring OB stars. The quality of the spectra is inadequate to rule out or confirm the presence of spectral lines. There is no indication of strong Fe lines at $6.4\,\mathrm{keV}$, as sometimes observed in SFRs (Takagi et al. 2002).

The spectrum is quite hard and can be fitted either with a thermal or an absorbed power-law model. The thermal plasma model fits best with a temperature of $200\,\mathrm{MK}$ (Table 4). Such a high temperature of interstellar gas within a small scale SFR cannot be plausibly explained. An absorbed power-law model, $K(E[\mathrm{keV}])^{-\gamma}$, where K is in photons $\mathrm{keV}^{-1}\mathrm{cm}^{-2}\mathrm{s}^{-1}$ at $1\,\mathrm{keV}$, fits best with $\gamma = 1.4 \pm 0.3$. This is a plausible value for the synchrotron emission spectrum. It prompts us to suggest that the relatively small volume at the west side of the SFR ON 2S is may be filled by synchrotron emission.

9. Discussion on the origin of the extended X-ray emission from ON2 S

The diffuse thermal X-ray emission in SFRs may result from a collection of unresolved point sources, cluster winds, and wind-blown bubbles. Non-thermal emission requires the acceleration of electrons, for which the diffuse shock acceleration (DSA) mechanism is often invoked. In this section, we discuss the applicability of these mechanisms to the diffuse X-ray emission from ON 2S.

9.1. Population of Point Sources

Unresolved X-ray emission from many low-mass YSOs present in a massive SFR can mimic diffuse emission. An underlying population of low-mass stars was invoked to explain the hard extended X-ray emission observed in the Orion and the Omega Nebula (Townsley et al. 2003; Güdel et al. 2008). The known massive YSOs in ON 2 are 10 000 yr old. At this age, low-mass YSOs are X-ray active, but may be undetected in 2MASS or IRAC images. From Fig. 5 we estimate that we can see ZAMS down to early G stars for $A_V = 0$, but with just $A_V = 10$ this is already restricted to late F types. To uncover a population of low-mass YSOs in ON 2 high-quality, sensitive near-IR (JHK)

Table 4: Parameters of thermal and non-thermal plasma models used to fit the spectra of diffuse emission in GAL 75.84+0.40 and in ON 2S (see Figs. 12, 14, 15)

GAL 75.84+0.40		
	Thermal plasma *tbabs*apec*	Non-thermal plasma *tbabs*powerlaw*
N_{H} [cm^{-2}]	$(4.0 \pm 0.3) \times 10^{22}$	$(4.8 \pm 0.6) \times 10^{22}$
	$kT = 2.8 \pm 0.3$ keV	$\gamma = 2.7 \pm 0.2$
F_{X}^{a} [erg cm^{-2} s^{-1}]	2×10^{-13}	
L_{X}^{b} [erg s^{-1}]	1×10^{32}	
ON 2S		
	Thermal plasma *tbabs*apec*	Non-thermal plasma *tbabs*powerlaw*
N_{H} [cm^{-2}]	$(1.3 \pm 0.2) \times 10^{22}$	$(1.2 \pm 0.3) \times 10^{22}$
	$kT = 17.7 \pm 9.6$ keV	$\gamma = 1.4 \pm 0.3$
F_{X}^{a} [erg cm^{-2} s^{-1}]	2×10^{-13}	
L_{X}^{b} [erg s^{-1}]	6×10^{31}	

[a] absorbed

[b] unabsorbed

imaging is needed.

Using results of Flaccomio et al. (2003) obtained from the study of stars in the Orion Nebula, we estimate that the X-ray luminosity of a 10 000 year old YSO with a mass of $0.5 \lesssim M/M_{\odot} \lesssim 1$ is $L_{\mathrm{X}} \approx 4 \times 10^{30}$ erg s^{-1}. Therefore, the presence of just ten such objects can easily explain the observed luminosity of the extended X-ray emission in ON 2S.

There are, however, arguments against interpreting the emission from ON 2S as being solely due to an unresolved population of YSOs. Firstly, as was discussed in Sect. 5, the *Spitzer* data confirm earlier suggestions that star formation occurred nearly simultaneously over this whole ON 2 SFR. The observed X-ray emission is so hard, that even if it were present in the areas with higher absorbing column we would still be able to detect it. Yet, the patch of hard diffuse X-ray emission is spatially confined. There is no reason to expect that low-mass YSOs are strongly clustered at a location that is away from the higher-mass YSOs.

Secondly, the spectrum from an unresolved population of YSOs would be much softer than what we observe in ON 2S. Townsley et al. (2003) used *Chandra* observations of the Omega and the Rosetta Nebulae to obtain a cumulative spectrum of YSOs. The absorbing columns to YSOs in these nebulae are similar to those we derive in ON 2S. Townsley et al. (2003) found that the cumulative spectrum of point sources can be well fitted with thermal plasma models with temperatures

not exceeding 3.1 keV. This is similar to what we infer from fitting the X-ray spectrum of GAL 75.84+0.40, but in ON 2S the temperatures are much higher (see Table 4).

Therefore, while it is possible that unidentified YSOs are embedded in ON 2, it appears that diffuse emission may also be present there.

9.2. Shocked Stellar Wind

The hot cluster winds filling the volumes of dense massive star clusters are driven by stellar winds and SNe (Chevalier & Clegg 1985). A cluster wind can be expected from a 4-6 Myr old massive cluster, such as Berkeley 87 (Oskinova 2005).

In essence, the X-ray luminosity and temperature of a wind from a cluster with the radius R_{cl} depends on the input of mechanical energy and mass. The multiwavelength observations of Berkeley 87 do not show any evidence of a recent SNR. Therefore, to crudely estimate the expected luminosity and temperature of the cluster wind from Berkeley 87, we consider only mechanic energy and mass input produced by stellar winds. In Berkeley 87 the wind energy production is dominated by the WR star WR 142. Recently, the stellar parameters of WR 142 were updated, and a mass-loss rate of $7 \times 10^{-6} M_{\odot} \mathrm{yr}^{-1}$, and wind velocity of 5500 km s^{-1} (or 4000 km s^{-1} allowing for stellar rotation) were derived (Oskinova et al. 2009).

To roughly estimate the energy input from other massive stars, we assume that there are ≈ 30 such stars in Berkeley 87 (see Section 3). The wind velocities of O and early B stars are in the range ≈ 1500–3000 km s^{-1}, while wind velocities of later B stars are in the range ≈ 300–1000 km s^{-1} (Lamers & Cassinelli 1999). Mass-loss diagnostics based on comprehensive stellar wind models that account for macro-clumping were recently used to infer empirical mass-loss rates of a few $\times 10^{-6}$ $M_\odot$yr^{-1} for typical O stars (Oskinova et al. 2007; Sundqvist et al. 2009). The mass-loss rates of later B-type stars are at least one order of magnitude smaller (Searle et al. 2008). The wind-energy input from the late B and A type stars can be neglected.

There are eight early-type OB giants and supergiants in Berkeley 87 (Massey et al. 2001). We assume that each of them has a terminal wind velocity of 2000 km s^{-1} and a mass-loss rate of 10^{-6} $M_\odot$yr^{-1}. Furthermore, we assume that there are 15 stars with terminal wind velocities of 600 km s^{-1} and mass-loss rates of 10^{-8} $M_\odot$yr^{-1} (corresponding to later B type stars). The cluster radius is 3 pc (Fig. 1).

Using scaling relations of Stevens & Hartwell (2003), the cluster wind luminosity is $L_X \approx 10^{44} \dot{M}_*^2 (R_{\rm cl} \bar{V}_*)^{-1}$ erg s^{-1}, and the cluster wind temperature is $T_X \approx 15 \bar{V}_*^2$ MK (accounting for the mass-loading from "cool" matter can lead to the somewhat lower temperature.). The dimension of $\dot{M}$ is $M_\odot$ yr^{-1}, $R_{\rm cl}$ is in pc, and $\bar{V}_*$ is in km s^{-1}. $\dot{M}_*$ is the sum of stellar mass-loss rates in the cluster, and $\bar{V}_*$ is the mean stellar wind velocity weighted by mass-loss rates. Using the wind parameters of the stars in Berkeley 87, a very hot ($T_X \sim 100$ MK) but faint ($L_X \lesssim 10^{30}$ erg s^{-1}) cluster wind emission can be expected. Note, that our estimates are not sensitive to the assumed wind parameters of the OB stars, because the kinetic energy of the WO wind alone is an order of magnitude higher that the combined kinetic energy input from all other stars.

Our *XMM-Newton* data do not show diffuse emission filling the cluster, with temperature peaking in the cluster center, and extending beyond its boarders, as predicted by the analytical models. Instead, we observe localized, small ($\lesssim 0.15$ pc^2) patches of diffuse emission within the cluster. Therefore, it is not possible to attribute the diffuse X-ray emission from ON 2S to the cluster wind.

If indeed the molecular cloud Onsala 2C and the adjacent star-forming region ON 2 are immediate neighbors of the cluster Berkeley 87, whose intra-cluster

medium is filled with hot tenuous wind, the situation may be analogous to the one considered by Cowie & McKee (1977) for the evaporation of a cool cloud in a hot gas. For a spherical cloud, the solutions of Cowie & McKee (1977) predict that the temperature rises steadily with the distance r from the cold cloud ($T \propto (1 - r^{-1})^{0.4}$) and the X-ray emission forms a "halo" around the cool cloud (see also Harper-Clark & Murray 2009). Broadly speaking, the thermal conduction would lower the temperature and increase the X-ray luminosity of the hot gas close to the interface (Steffen et al. 2008).

There are, however, a number of arguments against attributing the X-ray emission from ON 2S to the thermal evaporation of cool cloud material. The observed X-ray temperature at the interface between cool and hot gas appears to be unreasonably high (~ 200 MK). Moreover, the diffuse X-ray emission is localized in small areas, while the interface between cool and hot gas in Berkeley 87 extends over parsecs (see sketch in Fig. 2).

Furthermore, as noticed e.g. by Wang et al. (2006), the presence of the Fe-line complex at $\approx 6.4 - 6.7$ keV is a good indicator that cool cloud material is involved in the generation of X-rays. Wang et al. (2006) propose a cluster-cloud collision scenario, where the emission in Fe lines traces the shocked cloud gas. This line complex is very prominent in the Arches and the Quintuplet cluster spectra. Using the spectral parameters of the Fe-line complex obtained in Wang et al. (2006) we conclude that if Fe emission of comparable strength were present in ON 2S it would be noticeable even in our low S/N spectra. However, there is no indication for the presence of the Fe line complex in the X-ray spectra of ON 2S.

Thus, taking into account *i)* the spatial distribution of diffuse emission, *ii)* the very high temperature needed to fit a thermal model to the observed spectrum, and *iii)* the absence of fluorescent iron lines in the spectra, we conclude that the diffuse X-ray emission is *not* a consequence of the interaction of the cluster wind from Berkeley 87 with the cool cloud Onsala 2C.

Three massive stars (two BI and one OIII) are located just south from the area filled with extended X-ray emission (Fig. 8). The local interaction between the winds of these three stars may, in principle, lead to the heating of nearby regions. This scenario, however, is not confirmed by the data. As discussed in Section 8.1, the X-ray luminosity and spectrum extracted from the region around these three OB stars is domi-

nated by X-ray emission of BD+36°4032 and does not require any additional sources such as interactions between stellar winds.

Polcaro et al. (1991) reported the detection of strong diffuse emission around WR 142 in the optical. They argue that this diffuse emission likely originates in a supersonic flow centered on WR 142, and can be considered as evidence of a hot bubble around this star. Although theoretically expected, there is a dearth of detected diffuse X-ray emission from wind-blown bubbles around WR stars (Chu et al. 2003; Wrigge et al. 2005). The only two detected hot bubbles show a limb-brightened morphology and are extended on the scale of parsecs. The size of a hot bubble around WR 142, estimated using the classical work by Weaver et al. (1977), should be ≈ 40 pc or $\lesssim 1.5°$ at the distance of Berkeley 87. It should be noted, however, that Weaver et al. (1977) considered the case of an isolated star in a uniform medium, i.e. conditions that are clearly not valid for WR 142. A superbubble and super-shells can be expected around rich OB associations (Chu et al. 2003), such as Cyg OB 1, which comprises star clusters Berkeley 86, 87, IC 4996, and NGC 6913. However, these structures are extended over large scales of $\sim 10^2$ pc. The location of Berkeley 87 in the complex region of the Cygnus X superbubble makes the detection of an individual bubble around Berkeley 87 even more difficult.

Thus we conclude that stellar winds cannot be the main reason for the observed apparently diffuse emission.

9.3. Synchrotron Emission in Random Magnetic Fields

Diffuse hard X-ray emission with a power-law spectrum can be produced by the synchrotron mechanism. The latter requires the presence of energetic particles and magnetic fields.

It has been argued that the shocks in the cluster winds and/or colliding wind binaries efficiently accelerate electrons and protons to relativistic energies (Bykov et al. 2001; Quataert & Loeb 2005; Pittard & Dougherty 2006). The model calculations by Bednarek (2007) show that particles up to TeV energies should be present in Berkeley 87. These particles should be advected from the cluster on the time scale of $\sim 10^3$ yr. A simple scaling relations to estimate the expected surface brightness of the synchrotron emission from the cluster of massive stars were derived by

Quataert & Loeb (2005) and applied to the cluster in the central parsec of the Galaxy. Berkeley 87 is less rich than the Galactic Center cluster, but it contains WR 142, a WO star that alone has the wind kinetic energy $\approx 1.5 \times 10^{38}$ erg s^{-1}, making it comparable to the whole of the Galactic Center cluster. The small number of OB stars in Berkeley 87 results in the order of two lower UV luminosity, thus the cooling of particles by inverse Compton process is less significant. According to the scaling relations of Quataert & Loeb (2005), the surface brightness of Berkeley 87 in γ-rays is ~ 100 lower than that of the Central Cluster.

It is interesting to note that the winds from the dense group of three OB stars south of the ON 2S (see sketch in Fig. 2) may provide an additional source of particles accelerated *in situ* nearby to ON 2S.

To estimate at which distance from the stars the winds terminate and shock the H II gas, we consider a typical O star wind density profile which declines with distance as r^{-2}. The wind density close to the surface of an O star is $\sim 10^{10}$ cm^{-3}. For the typical ambient matter density, ~ 1 cm^{-3}, the stellar wind pressure would be equal to the ambient matter pressure roughly at the distance of the patch of diffuse X-ray emission (i.e 0.3 pc away from OIII star BD+36°4032).

Recently, Bykov et al. (2008) addressed the effect of a random magnetic field on synchrotron emission. In was shown (in the context of young supernova remnants) that prominent localized structures can appear in synchrotron maps of extended sources with random magnetic fields, even if the particle distribution is smooth. The bright structures originate as high-energy electrons radiate efficiently in local enhancements of the magnetic field. The size of the "patch" of hard X-ray emission in ON 2S is about 0.1 pc^2. This could be relevant in the framework of the Bykov et al. model if the shock velocity is a few×10^3 km s^{-1} (Bykov A., priv. communication). This is a plausible number for a stellar as well as for a cluster wind.

Magnetic fields, along with turbulence, play a leading role in star formation (Crutcher et al. 2009). The field strengths (50-700 μG) of an order, or even two, higher than the field in the diffuse ISM are detected in SFRs, moreover the field geometry is shown to be far from uniform (Schleuning 1998). These measurements provide strong support to the idea that magnetic fields of similar strengths can be present in other, if not all, SFRs, with ON 2S being no exception. Ferland (2009) reviewed several recent observational studies of the relationships between magnetic fields, stellar feed-

Table 5: High-mass SFRs where hard diffuse X-ray emission was detected[a]

Region	L_X [10^{32} erg s^{-1}]	N_H [10^{22} cm^{-2}]	Size [pc]	Distance [kpc]	thermal[b] [keV]	power law Γ	Comment[c]	Reference
Orion	0.6	0.1	2	2.6	0.4		point sources (?)	(1)
ON 2 S	0.4	1.5	0.1	1.2	18	≈ 1.4	point sources, synchrotron (?)	(2)
GAL 75.84+0.40	0.4	4.6	0.1	1.2	3	≈ 2.6	point sources (?)	(2)
RCW 38	1	1	1.5	≈ 2	1.7	≈ 2.8		(3)
NGC 6334	0.1-5	0.5-10	1	1.7	> 1			(4)
Westerlund 1	300	2	10	5	≥ 3		IC (?)	(5)
NGC 3603	200	0.7	4	7	3			(6)
Arches	200	10	3	8.5	5.7			(7)
Sgr B2	9	40	0.2	8.5	10			(8)
W49A	30	50	0.3	11.4	7			(9)
LMC 30 Dor C	10^4	0.1	10	50		≈ 2.5	superbubble	(10)
LMC N11	1.5×10^3	0.5	10	50		≈ 1.7	superbubble	(11)
LMC N51D	4×10^3	0.03		50		≈ 1.3	superbubble	(12)

[a] All numbers in this Table are approximate. The reader is urged to consult the original publications describing these complex objects and their observations in detail.

[b] Temperature of the hardest component in multi-temperature spectral fits

[c] Comment on the properties of suspected non-thermal X-ray emission, if any

(1) Güdel et al. (2008); (2) this work; (3) Wolk et al. (2002): (4) Ezoe et al. (2006); (5) Muno (2003);
(6) Moffat et al. (2002); (7) Yusef-Zadeh et al. (2002); (8) Takagi et al. (2002); (9) Tsujimoto' et al. (2006);
(10) Bamba et al. (2004); (11) Maddox et al. (2009); (12) Cooper et al. (2004);

back, and the geometry of H II regions. The observations reveal that magnetic field lines can be preferentially aligned perpendicular to the long axis of the quiescent cloud before stars form. After star formation and push-back occurs, ionized gas will be constrained to flow along the field lines and escapes from the system in directions perpendicular to the long axis. Wave motions may be associated with the field and so could contribute a turbulent component to the observed line profiles.

It appears that all ingredients required to produce a small bright patch of synchrotron radiation in the X-ray image may be present in ON 2S. The particles accelerated up to TeV energies may result from the shocked cluster winds and/or from the YSO outflows. Sufficiently strong turbulent magnetic fields may be present in the vicinity of star forming regions. In addition, the presence of clumps of matter would enhance the surface brightness of the radiation (Bykov et al. 2008), and such clumps of matter are present in the radio maps of the region (Shepherd et al. 1997). To summarize, a synchrotron emission may be expected from the region where the strongly shocked stellar winds and turbulent magnetic fields co-exist.

10. Comparison with other SFRs

In Table 5 we expand the list compiled by Tsujimoto' et al. (2006) to summarize the properties of high-mass star forming regions with detected hard diffuse X-ray emission.

It can be immediately seen that the properties of SFRs in Table 5 are quite diverse. It appears that three broad categories can be distinguished. The superbubbles around large clusters and associations of massive stars belong to one of these categories. Large spatial scale (10–100 pc), high luminosity, and often limb brighten morphology are characteristic for objects such as 30 Dor C, LMC N11, LMC N51D. The star clusters blowing cluster winds belong to the second category. The examples include Westerlund 1, the Arches, and NGC 3603. Although their X-ray emission is hard, it can, usually be fitted with hot ($T_X \lesssim 30$ MK) thermal plasma. The diffuse X-rays fill the cluster interior on the scale of a few pc. In the third group, where, as we believe ON 2 belongs, small scale areas (~ 0.1 pc) are filled with diffuse X-rays. In such SFRs as ON 2, RCW 38, WR 49A, or Sgr 2, the hot ($T_X \gtrsim 100$ MK) or non-thermal plasma is found in immediate vicinity of UCH II regions. While Takagi et al. (2002) and Güdel et al. (2008) suggest that hard X-rays may originate from unresolved populations of low-mass pre-main sequence stars, we suggest, that at

least in some objects, the non-thermal emission may be expected from interactions between magnetic fields and the particle accelerated in shocked stellar winds.

It is interesting to note that the distribution of hard extended X-ray emission in the two closest SFRs – Orion nebula and ON 2S – is somewhat similar: diffuse X-ray emission filling a cavity seen in the IR images, slightly offset from a small group of massive stars. The X-ray spectrum, however is noticeably harder in the case of ON 2S.

11. Concluding remarks

Throughout the paper we adopted the distance $d = 1.23$ kpc to both the young massive star cluster Berkeley 87 and the SFR ON 2. This assumption has allowed us to propose physical interaction between the radiative and mechanical feedback from OB stars in Berkeley 87 and the observed diffuse X-ray emission in the regions of active star formation.

In the majority of papers published on the SFR ON 2, a distance in excess of 4 kpc is adopted. In this case, there would be no physical connection between the massive star cluster and the SFR. The X-ray luminosities and the areas filled with X-ray emission would be factor of $\gtrsim 16$ larger. The results of our spectral analysis would, however, not been affected.

To summarize, we have conducted *XMM-Newton* observations of the massive star-forming region ON 2. The observations and their subsequent analysis have shown:

1. Diffuse X-ray emission on a cluster scale, which might have been expected to result from the cluster wind and wind blown bubble in Berkeley 87, was not detected.

2. From a literature search we do not confirm previous reports of γ-ray emission from Berkeley 87.

3. The northern (ON 2N) and the southern (ON 2S) parts of the star forming complex ON 2 are bright sources of diffuse X-ray emission.

4. X-ray images of ON 2N show that X-ray emission fills the interior of the compact H II region GAL 75.84+0.40. This emission is diffuse and strongly absorbed, indicating that it originates from deeply embedded sources. We rule out the ionizing stars of the H II region as its origin, and speculate that it can result from an embedded cluster of young low mass stars.

5. In ON 2S the extended X-ray emission traces the eastern edge of this SFR. This extended emission consists of point sources superimposed on or immersed in diffuse emission.

6. We discuss different possible scenarios to explain the apparently diffuse emisson from ON 2S, such as cluster wind, synchrotron radiation, and unresolved point sources. We favor the last two options as the most probable explanations.

A. On the absence of detected γ-ray emission from Berkeley 87

It has long been realized that young massive stellar associations can be potential sources of cosmic- and γ-rays, where the acceleration of particles occurs in the shocks produced by turbulent interactions of supersonic stellar winds (Montmerle 1979; Cassé & Paul 1980; Cesarsky & Montmerle 1983). Berkeley 87 is a testbed for the models of γ-ray production due to its proximity, relatively high space density of massive stars, and, chiefly, due to the cluster membership of WR 142 – the star with perhaps the most powerful stellar wind in the Galaxy.

However, our careful check revealed that in contrast to the reports in the literature, the high-energy emission from Berkeley 87 was not previously observed.

We were not able to confirm the detection of diffuse X-ray emission from Berkeley 87 by *EXOSAT* as referenced by Bednarek (2007). Berkeley 87 was observed $\sim$ 1 deg off-axis. There is no reference in the literature to the detection of Berkeley 87 or any object within its boarders by *EXOSAT*. Similarly, no detection of Berkeley 87 by *ASCA* was ever reported. Roberts et al. (2002) report the identification of an ASCA X-ray source coincident with the EGRET γ-ray source 2CG 075+00, GeV J2020+3658 or 3EG J2021+3716 as the young radio pulsar PSR J2021+3651, which is located at a distance of $\approx$ 10 kpc. The pulsar and its associated pulsar wind nebula G75.2+0.1 are $\approx$ 28' away from the outer border of Berkeley 87.

Bednarek (2007) considered two *EGRET* sources, 3EG J2016+3657 and "3EG J2021+4716" , as related to Berkeley 87 cluster. The elliptical fits to the 95% confidence position contours of all 3EG EGRET sources are presented in Mattox et al. (2001). The smallest separation of the outer border of Berkeley 87 from 95% confidence position contours of 3EG J2016+3657 is $\approx$ 30'. No source "3EG J2021+4716" is present in the 3EG catalog (Hartman et al. 1999).

Aharonian et al. (2006) report that the observations of Berkeley 87 region yielded only upper limits that are a factor of $\lesssim$3 lower than TeV fluxes expected from an OB stellar association. The Milagro group (Abdo et al. 2007) reported the detection of an extended TeV source MGRO J2019+37, but their analysis favors its associations with the PSR J2021+3651 and its pulsar wind nebula G75.2+0.1.

From our literature search, we conclude that prior to our *XMM-Newton* observations, there were no firm detection of X-ray diffuse sources from Berkeley 87. We also conclude that there are no γ-ray source identifications within Berkeley 87.

A. Note added in Proof

New *Chandra* X-ray telescope observations of a part of Berkeley 87 became public after this article had been accepted. The *Chandra* exposure is less sensitive than the *XMM-Newton* observations discussed in the present paper, but has a superior angular resolution of $\lesssim$1″. The new *Chandra* images reveal three discrete sources in the region termed D in Figs. 13, 15. According to a first analysis, the *Chandra* spectra of these three point sources correspond to strongly absorbed thermal emission with $N_H \approx 3 \times 10^{22}$ cm^{-2} and $kT \approx 2$ keV. Such parameters are usual for YSOs as discussed in Section 9.1. Hence the new data indicate that unresolved point sources contribute to the apparently diffuse emission from ON 2S detected by *XMM-Newton*, confirming what we have discussed in Section 9 as one possibility. However, the sum of the fluxes from the discrete sources is about three times smaller than the flux from the whole region D as measured with *XMM-Newton*, still leaving open the question about the true nature of the major part of extended emission observed with *XMM-Newton*.

REFERENCES

Abdo, A. A. et al. 2007, ApJ, 658, L33

Aharonian, F. et al. 2006, A&A, 454, 775

Allen, L. E., et al. 2004, ApJS, 154, 363

Arnaud, K. A. 1996, ASP Conf. Ser. Vol. 101. Astron. Soc. Pac, San Francisco, p.17

Bamba, A. et al. 2004, ApJ, 602, 257

Bohlin, R. C. & Savage, B. D. 1981, ApJ, 249, 109

Bednarek, W. 2007, MNRAS, 382, 367

Bessell, M. S., & Brett, J. M. 1988, PASP, 100, 1134

Brogan, C. L. & Troland, T. H. 2001, ApJ, 560, 821

Bykov, A. 2001, Space Sci. Rev., 99, 317

Bykov, A. M., Uvarov, Y. A., & Ellison, D. C. 2008, ApJ, 689, L133

Cardelli, J.A., Clayton, G.C., & Mathis, J.S. 1989, ApJ, 345, 245

Cassé, M. & Paul, J.A. 1980, ApJ, 237, 236

Cesarsky, C.J. & Montmerle, T. 1983, Space Sci. Rev., 36, 173

Chevalier, R. A. & Clegg, A. 1985, Nat, 317, 44

Chu, Y.-H., Guerrero, M. A., Gruendl, R. A., Garcia-Segura, G., & Wendker, H.L. 2003, ApJ, 599, 1189

Cooper, R. et al. 2004, ApJ, 605, 751

Cowie, L. L. & McKee, C. F. 1977, ApJ, 211, 135

Crutcher, R. M., Hakobian N., & Troland, T. H. 2009, ApJ, 692, 844

Dent, W.R.F., Macdonald, G.H., & Andersson, M. 1988, MNRAS 235, 1397

Ezoe, Y., Kokubun, M., Makishima, K., Sekimoto, Y., & Matsuzaki, K. 2006, ApJ, 638, 860

Fazio, G., et al. 2004, ApJS, 154, 10

Ferland, G. J. 2009, IAUS, 259, 25

Flaccomio, E., Damiani, F., Micela, G., Sciortino, S., Harnden, F. R. Jr, Murray, S. S., & Wolk, S. J. 2003, ApJ, 582, 398

Garay, G., Rodriguez, L.F., Moran, J.M., & Churchwell, E. 1993, ApJ, 418, 368

Gruendl, R. A., & Chu, Y.-H. 2009, ApJS, 184, 172

Güdel, M., Briggs, K.R., Montmerle, T., Audard, M., Rebull, L., & Skinner, S.L. 2008, Science, 319, 309

Hamann, W.-R. & Gräfener, G. 2004, A&A, 427, 697

Harper-Clark, E. & Murray, N. 2009, ApJ, 693, 1696

Hartman, R.C., et al. 1999, ApJS, 123, 79

Harvey, P. M., et al. 2006, ApJ, 644, 307

Hofner, P. & Churchwell, E. 1996, A&AS, 120, 283

Kozłowski, S., & Kochanek, C. S. 2009, ApJ, 701, 508

Maddox, L.A., Williams, R.M., Dunne, B.C., & Chu, Y.-H 2009, ApJ, 699, 911

Massey, P., DeGioia-Eastwood, K., & Waterhouse, E. 2001, AJ, 121, 1050

Mathys, G. 1987, A&AS, 71, 201

Matthews, H.E., Goss, W.M., Winnberg, A., & Habing, H.J. 1973, A&A, 29, 309

Matthews, N., Anderson, M., & MacDonald, G.H. 1986, A&A, 155, 99

Mattox, J., Hartman, R.C., & Reimer, O. 2001, ApJS, 135, 155

Meynet, G. & Maeder, A. 2005, A&A, 429, 581

Moffat, A.F.J., et al. 2002, ApJ, 573, 191

Moneti, A., Stolovy, S., Bommart, J. A. D. L, et al. 2001, A&A, 366, 106

Montmerle, T., 1979, ApJ, 231, 95

Muno, M.P., et al. 2003, ApJ, 589, 225

Negueruela, I. 2004, AN, 325, 380

Lamers, H. J. G. L. M. & Cassinelli, J. P. 1999, Introduction to Stellar Winds (Cambridge: Cambridge Univ. Press)

Levesque, E.M., Massey, P., Olsen, K.A.G., Plez, B., Josselin, E., Maeder, A., & Meynet, G., 2005, ApJ, 628, 973

Oskinova, L.M. 2005, MNRAS, 361, 679

22

Oskinova, L. M., Hamann, W. R., & Feldmeier, A. 2007, A&A, 476, 1331

Oskinova, L.M., Hamann, W.-R., Feldmeier, A., Ignace, R., & Chu, Y.-H. 2009, ApJ, 693, L44

Palagi, F., Cesaroni, R., Comoretto, G., Felli, M., Natale, V., 1993 A&AS, 101, 153

Pittard, J. M. & Dougherty, S. M. 2006, MNRAS, 372, 801

Polcaro, V.F., Giovannelli, F., Manchanda, R. K., Norci, L., & Rossi, C. 1991, A&A, 252, 590

Pravdo, S.H., Tsuboi, Y., Suzuki, Y., Thompson, T.J., Rebull, L. 2009, ApJ, 690, 850

Quataert, E. & Loeb, A., 2005, ApJ, 635, L45

Reifenstein, E.C., Wilson, T.L., Burke, B.F., Mezger, P.G., & Altenhoff, W.J. 1970, A&A, 4, 357

Roberts, M.S.E. et al. 2002, ApJ, 577, L19

Sundqvist, J. O., Puls, J., & Feldmeier, A. 2009, arXiv 0911.3361S

Schaller G., Schaerer D., Meynet G., Maeder A. 1992, A&AS, 96, 269

Schneider, N., Simon, R., Bontemps, S., Comerón, F., & Motte, F. 2007, A&A 474, 873

Schleuning, D. A. 1998, ApJ, 493, 811

Searle, S. C., Prinja, R. K., Massa, D., & Ryans, R. 2008, A&A, 481, 777

Shepherd, D.S., Churchwell, E., & Wilner, D.J. 1997, ApJ, 482, 355

Skrutskie, M. F., et al. 2006, AJ, 131, 1163

Steffen, M., Schönberner, D., Warmuth, A. 2008, A&A, 489, 173

Stevens, I.R. & Hartwell, J.M. 2003, MNRAS, 339, 280

Takagi, S., Murakami, H., & Koyama, K. 2002, ApJ, 573, 275

Townsley, L.K., Feigelson, E.D., Montmerle, T., Broos, P.S., Chu, Y.-H., & Garmire, G.P. 2003, ApJ, 593, 874

Tsujimoto, M., Hosokawa, T., Feigelson, E.D., Getman, K.V., & Broos, P.S. 2006, ApJ, 653, 409

Turner, D. G. & Forbes, D. 1982, PASP, 94, 789

Turner, D. G., Rohanizadegan, M., Berdnikov, L. N., & Pastukhova, E.N. 2006, PASP, 118, 1533

Uyaniker, B., Fürst, E., Reich, W., Aschenbach, B., & Wielebinski R. 2001, A&A, 371, 675

Vanbeveren, D., de Donder, E., van Bever, J., van Rensbergen, W., & de Loore C. 1998, New Astron., 3, 443

Weaver, R., McCray, R., Castor, J., Shapiro, P., & Moore, R. 1977, ApJ, 218, 377

Wang, Q. D., Dong, H., & Lang, C. 2006, MNRAS, 371, 38

Wink, J. E., Altenhoff, W. J., & Mezger, P.G. 1982, A&A, 108, 227

Wolk S. J., Bourke T. L., Smith R. K., Spitzbart B., & Alves, J., 2002, ApJ, 580, L161

Wrigge, M., Chu, Y.-H., Magnier, E.A., & Wendker, H.J. 2005, ApJ, 633, 248

Yusef-Zadeh, F., Law, C., Wardle, M., Wang, Q. D., Fruscione, A., Lang, C. C., & Cotera, A. 2002, ApJ, 570, 665